Solar System Research, Vol. 36, No. 5, 2002, pp. 367–373. Translated from Astronomicheskii Vestnik, Vol. 36, No. 5, 2002, pp. 395–402.

The Effect of the Shape of Dust Aerosol Particles in the Martian Atmosphere on the Particle Parameters

Zh. M. Dlugach*, M. I. Mishchenko, and A. V. Morozhenko***

** Main Astronomical Observatory, National Academy of Sciences of Ukraine, Goloseevo, Kiev, 03680 Ukraine*

*** NASA Goddard Institute for Space Studies, 2880 Broadway, New York 10025, USA*

Received November 19, 2001; in final form, February 4, 2002

Abstract—The influence of the shape of dust aerosol particles in the Martian atmosphere on the imaginary part of the refractive index n_i as derived from photometric observations during the period of the highest activity of the dust storm in 1971 was studied and exemplified for particles of spherical and oblate spheroidal shape. A similar analysis was performed for mean particle radii r_0 and optical thicknesses τ_0 of the dust layer estimated from polarization observations for periods of high atmospheric transparency. It was demonstrated that the values obtained for these optical parameters are affected by the adopted aerosol shape. Namely, the values of n_i, r_0, and τ_0 found for spheroidal particles proved to be nearly twice as large as those for spheres. However, they are still much less than the available estimates of these parameters inferred, in particular, from interpreting space experiments. The reason for this difference needs further investigation.

INTRODUCTION

It has been demonstrated in our previous studies (Dlugach and Morozhenko, 2000, 2001) that the sizes of Martian dust particles, the imaginary parts of their complex refractive index, and the optical thicknesses of the atmosphere of Mars for periods of its high transparency differ by a factor of ten or more if estimated by different methods. A lot of explanations can be suggested for this, in particular, the nonuniqueness of solutions to inverse multiparameter problems, the use of different assumptions about the shape of dust particles, and so on. For example, a model of spherical particles was considered by Morozhenko (1974), Dollfus *et al.* (1974), and Dlugach and Morozhenko (2000, 2001), whereas Pollack *et al.* (1977, 1995) and Petrova (1999) analyzed observational data assuming the aerosol to be nonspherical. The goal of the present study is to try to examine the influence of the aerosol shape on estimates of the above-listed atmospheric optical parameters as derived from analyzing surface polarization and photometric observations. The gamma distribution

$$f(r) = \mathrm{const}\, r^{(1-3b)/b} \exp\left(-\frac{r}{ab}\right), \tag{1}$$

the lognormal distribution

$$f(r) = \mathrm{const}\, r^{-1} \exp\left[-\frac{\ln^2 r/r_0}{2\sigma^2}\right] \tag{2}$$

and the modified power law

$$f(r) = \begin{cases} \mathrm{const}, & 0 \le r \le r_1 \\ \mathrm{const}\, r^{-\zeta}, & r_1 \le r \le r_2 \\ 0, & r > r_2. \end{cases} \tag{3}$$

are used for a particle size distribution function.

IMAGINARY PART OF REFRACTIVE INDEX

The values of the imaginary part of the refractive index n_i obtained in our previous studies (Dlugach and Morozhenko, 2000, 2001) for the range of wavelengths from 0.260 to 0.717 μm are given in Table 1. They are based on measurements of the Martian visible albedo at a phase angle $\alpha = 42°$ performed during the period of the highest activity of the dust storm in 1971 (Aleksandrov *et al.*, 1977; Caldwell, 1977). Now, we shall try to evaluate how sensitive these estimates are to the choice of particle shape. Remember that in the above-mentioned studies we used a model of a semi-infinite dust layer consisting of *spherical* particles with the lognormal size distribution (2). The real parts of the refractive index n_r were taken from laboratory measurements for basalt glass (Pollack *et al.*, 1973) and are also presented in Table 1. Such a choice was based on the fact that, according to surface polarimetric observations, $n_r = 1.59 \pm 0.01$ during the maximum of the 1971 dust storm (Dollfus *et al.*, 1974). These estimates are very close to the values of n_r for basalt glass (1.57). One can suggest that, if the refractive indices of the Martian dust particles and of the above-mentioned mineral have similar real parts, their imaginary parts cannot differ greatly. The measured values $n_i^{\mathrm{bas\ gl}}$ of the imagi-

0038-0946/02/3605-0367$27.00 © 2002 MAIK “Nauka / Interperiodica”

Table 1. Optical parameters of dust particles

λ, µm	0.260	0.308	0.336	0.366	0.433	0.536	0.654	0.717
$A(42°)$	0.012	0.016	0.017	0.027	0.052	0.108	0.219	0.256
n_r	1.62	1.60	1.59	1.58	1.57	1.57	1.57	1.57
n_i	0.0025	0.0013	0.0013	0.0010	0.00071	0.00038	0.00014	0.00010
$n_i^{\text{bas gl}}$	0.068	0.020	0.0071	0.0023	0.00064	0.00046	0.00045	0.00058
n_r'		1.48	1.49	1.50	1.51	1.51	1.51	1.51
n_i'		0.038	0.038	0.037	0.026	0.008	0.003	0.003

nary part of the refractive index for basalt glass (Pollack *et al.*, 1973) are also given in Table 1.

The visible albedo $A(\alpha)$ was calculated by the formula

$$A(\alpha) = \frac{2}{\pi}\int_{\alpha-\frac{\pi}{2}}^{\frac{\pi}{2}}\int_{0}^{\frac{\pi}{2}}\rho(\mu, \mu_0, \varphi)\mu\mu_0\cos\psi d\omega' d\psi, \quad (4)$$

where $\rho(\mu, \mu_0, \varphi)$ is the reflection coefficient of the semi-infinite layer (calculated via the method suggested by Dlugach and Yanovitskij (1974)), ψ and ω'– are the planetocentric coordinates related to μ (the cosine of the angle of reflection) and μ_0 (the cosine of the angle of incidence of solar radiation) by the relations

$$\begin{aligned} \mu_0 &= \cos\psi\cos(\alpha - \omega'), \\ \mu &= \cos\psi\cos\omega'. \end{aligned} \quad (5)$$

At the first stage, for a wavelength of 0.433 µm, assuming that n_r = 1.57 and that n_i corresponds to 0.00071, which is the average value for basalt and basalt glass (Pollack *et al.*, 1973), we found that our measurements and calculations agree best for r_0 = 4.5 µm and σ^2 = 0.2 in the lognormal law (2) (r_{eff} = 7.4 µm, ν_{eff} = 0.22 for the gamma distribution (1)). Then, by fitting the measured and calculated values of $A(42°, \lambda)$ for this radius, we found the spectral values of the imaginary part of the refractive index $n_i(\lambda)$. It can be seen from the table that the obtained estimates of n_i and the corresponding values of the imaginary part of the refractive index for basalt glass agree fairly well only in the visible region of the spectrum; they are much less consistent in the UV and IR ranges. This discrepancy can, at least partly, be explained for the UV region by the actually existing vertical stratification of cloud particles according to their size (Morozhenko, 1995a, 1995b). The point is that in the optically thick atmosphere diffusely reflected radiation is formed at some effective optical depth τ_{eff}, which is proportional to $[1 - \omega(\lambda)]^{-1/2}$. This means that, in the case of a dust storm on Mars, when the visible albedo decreases considerably with decreasing wavelength, the value of τ_{eff} must also diminish with the decrease in wavelength; i.e., the diffusely reflected ultraviolet radiation is generated higher in the atmosphere than the infrared radiation. As indicated by Morozhenko (1995a, 1995b), during a dust storm the particle radius decreases with height, and therefore the actual value of r_0 in the UV region must be less than the value r_0 = 4.5 µm, which we obtained. Our neglect of this fact must certainly result in an underestimation of the imaginary part of the refractive index in the UV spectral region. However, this explanation has nothing to do with our estimates of n_i for the IR region, since in this case we would overestimate the values of the imaginary part.

In addition, we also presented in Table 1 for comparison the values of real n_r' and imaginary n_i' parts of the refractive index for the Martian dust particles as derived by Ockert-Bell *et al.* (1997) from analyzing observations of the reflectance of the bright Amazonis area. Notice a very great (of an order or more) difference between the estimates obtained for the imaginary part of the refractive index. One can naturally ask what this results from. Note that a weak point of our study was the application of the model of spherical particles, and one is tempted to consider this factor responsible for the difference obtained. Hereafter, we shall try (within the limits of possibility) to estimate the influence of the particle shape on the value of the imaginary part of the refractive index.

A rigorous calculation of the elements of the light scattering matrix for nonspherical particles with sizes belonging to the so-called resonance region (that is, covering the wavelengths that do not differ greatly from the incident radiation) is a very complicated problem. At present, the so-called Waterman's T-matrix approach (see Mishchenko *et al.*, 1996 for details) is one of the most developed and widely used tools for strict computations of scattering by such particles, and there is a corresponding code available, which is freeware (Mishchenko and Travis, 1998; http://www.giss.nasa.gov/@crmim). Taking into account the available computer facilities, we adopted the following model of nonspherical particles: randomly oriented oblate spheroids (the aspect ratio ε = 2) with sizes distributed according to the modified power law (3) at $\xi = 3$ with $r_{eff} = 1.5$ and $\nu_{eff} = 0.2$ [for more details concerning the choice of size distribution function in such computations see (Mishchenko *et al.*, 1996)]. The particle shape was chosen for two reasons: (1) computations for such particles have been already performed (Petrova, 1999), and (2) from simulations of dust storm processes on Mars Murphy *et al.* (1990) concluded that dust particles of this shape can be contained in the dust clouds.

As an example, in Fig. 1 we presented the first elements of the scattering matrix F_{11} (the scattering phase function) computed at $n_r = 1.50$, $n_i = 0.001$, and $\lambda = 0.35$ μm for scattering angles γ from 100° to 180° for the abovementioned spheroids (pluses) and for spheres (oblique crosses) with similar parameters of size distribution function. It can be seen that, for example, for $\gamma = 140°$ ($\alpha = 40°$), the phase scattering functions differ by about a factor of two. Therefore, it is interesting to examine how this difference in the phase scattering functions affects the reflective properties of the dust layer, in particular, a single-scattering albedo, and, consequently, the imaginary part of the refractive index of dust particles. Comparing the observational results for $A(42°, \lambda)$ (the first row in Table 1) with the values of the Martian visible albedo (in the model of the semi-infinite dust layer) calculated for the adopted model of spheres and spheroids, we obtained the spectral values of single-scattering albedos $\omega^{(1)}$, $\omega^{(2)}$ and of imaginary parts of the refractive index $n_i^{(1)}$ (for spheres) and $n_i^{(2)}$ (for spheroids) in the spectral range 0.366–0.717 μm, which are presented in Table 2. It can be seen that the imaginary parts also differ, as a maximum, by about a factor of 2. In addition, we used (4) to calculate the values of $A(\alpha)$ at α = 0°, 10°, 20°, 30°, and 40° for the abovementioned model of spheroids ($n_i^{\text{spheroids}} = 0.001$) and spherical particles with different n_i and then found at which values of the imaginary part n_i the values of $A(\alpha)$ for the spherical particles are equal to those obtained for the spheroids (at $n_i^{\text{spheroids}} = 0.001$). It turned out that

α, deg	0	10	20	30	40
n_i^{spheres}	0.0016	0.0025	0.0017	0.0008	0.0007

We can see that in this case the imaginary parts for spheres and spheroids differ by a factor of 2.5 as a maximum.

Thus, considering spheres and spheroids, we can conclude that the shape adopted for dust particles is important in estimating the imaginary part of their refractive index from observations of the visible albedo of Mars. However, its effect is not strong enough to be responsible for the difference of an order of magnitude or greater, which is precisely the difference that was found between the imaginary parts obtained by Pollack *et al.* (1995), Ockert-Bell *et al.* (1997), and Dlugach and Morozhenko (2001) (see Table 1). Unfortunately, it is difficult to predict the behavior of larger particles. However, the computations performed by Mishchenko *et al.* (1996) for oblate spheroids with x_{eff} ($x_{eff} = 2\pi r_{eff}/\lambda$) varying up to 30 demonstrate that in the large-size region the difference between the scattering phase functions for spheres and for spheroids is nearly constant for scattering angles from 130° to 150°. We want to emphasize once more that, as stated above, a rigorous calculation of the elements of the scattering matrix for polydisperse systems of nonspherical particles with sufficiently large effective sizes is a very complicated problem, and, so far, its solution is impossible in many cases.

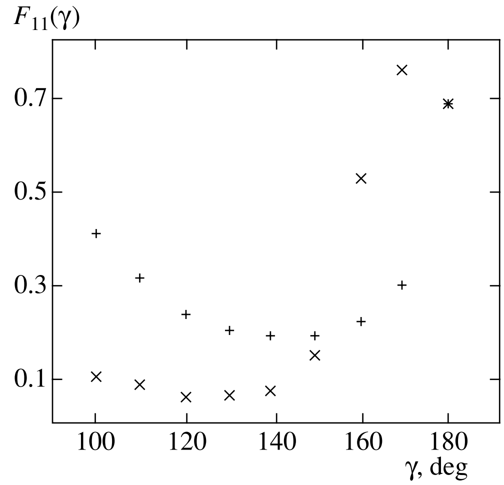

Fig. 1. Scattering phase functions calculated for spheres (oblique crosses) and oblate spheroids (pluses) distributed in size by the modified power law (3) for λ = 0.35 μm at $n_r = 1.50$, $n_i = 0.001$, $r_{eff} = 1.5$, $\nu_{eff} = 0.2$.

In closing this section, let us mention that the same observational data on $A(42°, \lambda)$ were used by Dlugach (1978) in order to find, in particular, the imaginary part of the refractive index. A model of a semi-infinite dust layer consisting of spherical particles with $r_0 = 10$ μm was adopted, but the scattering phase function for this system of particles was corrected (for scattering angles

Table 2. Imaginary part of refractive index for dust particles with a modified power law size distribution at $r_{eff} = 1.5$ μm and n_r =1.50

λ, μm	0.366	0.433	0.536	0.654	0.717
			Spheres		
$\omega^{(1)}$	0.73	0.84	0.925	0.979	0.985
$n_i^{(1)}$	0.009	0.004	0.0015	0.0004	0.00027
			Spheroids		
$\omega^{(2)}$	0.61	0.76	0.89	0.968	0.979
$n_i^{(2)}$	0.020	0.0072	0.0025	0.0006	0.0004

from 100° to 180°) so that the calculated phase function gave the best possible fit to the function observed on the *Mariner 9* spacecraft in November 1971 in the photometric band *V* (Thorpe, 1973). Namely, the corrected phase scattering function did not demonstrate a strong backscattering typical of spherical particles. Eventually, it was obtained that $10^{-3} \geq n_i \geq 5 \times 10^{-5}$ in the spectral range 0.360–0.717 μm; the values are close to our estimates presented in Table 1.

PARTICLE RADIUS AND OPTICAL THICKNESS OF DUST LAYER DURING PERIODS OF HIGH ATMOSPHERIC TRANSPARENCY

Minimum values of the dust particle radius and of the optical thickness of the layer for the clear Martian atmosphere were obtained from the results of polarization measurements (Morozhenko, 1969, 1974) using a model of *spherical nonabsorbing particles with a spectrally invariable real part of the refractive index*. It was assumed in the papers cited above that the angle of polarization inversion for the underlying surface α_i^s is independent of the wavelength, and a reduction of the angle of inversion observed in the short wavelength region of the spectrum ($\lambda < 0.450$ μm) is associated only with atmospheric scattering. For an optically thin layer of gas and aerosols (that is, with allowance for the first-order scattering only) the following expression is true for the product of polarization *P* by the visible planetary albedo *A*:

$$\begin{aligned} B(\alpha, \lambda) &= P(\alpha, \lambda)A(\alpha, \lambda) \\ &= -\frac{\omega_0(\lambda)}{2\pi}[\beta(\lambda)Q_R(\pi-\alpha) + (1-\beta(\lambda)) \\ &\quad \times Q_a(\pi-\alpha)] \int_{\alpha-\pi/2}^{\pi/2} d\omega \int_0^{\pi/2} \frac{\mu\mu_0}{\mu+\mu_0} \qquad (6) \\ &\quad \times \left[1 - \exp\left\{-\tau_0\left(\frac{1}{\mu} + \frac{1}{\mu_0}\right)\right\}\right] \cos\psi d\psi - \frac{2}{\pi} Q_s(\alpha, \lambda) \\ &\quad \times \int_{\alpha-\pi/2}^{\pi/2} d\omega \int_0^{\pi/2} \mu\mu_0 \exp\left[-\tau_0\left(\frac{1}{\mu} + \frac{1}{\mu_0}\right)\right] \cos\psi d\psi, \end{aligned}$$

Here, Q_R is the second element of the scattering matrix in the Rayleigh case, Q_a is the second element of the scattering matrix as calculated for the given refractive index and size distribution function of the particles, and Q_s is the second element of the Stokes vector for the surface. Moreover,

$$\beta(\lambda) = \frac{\tau_g(\lambda)}{\tau_g(\lambda) + \tau_a(\lambda)}, \qquad (7)$$

$$\omega_0(\lambda) = \frac{1}{1 + \left(\frac{1}{\omega_a} - 1\right)(1-\beta)}, \qquad (8)$$

$$\omega_a(\lambda) = \frac{q_{sc}(\lambda)}{q_e(\lambda)}, \qquad (9)$$

where $q_{sc}(\lambda)$ and $q_e(\lambda)$ are the scattering and extinction coefficients for the polydisperse medium, and τ_g and τ_a are the optical thicknesses for gaseous and aerosol components of the atmosphere. Obviously, the second term in formula (6) vanishes at the inversion point.

Morozhenko (1974) used observations of $B(\alpha, \lambda)$ obtained at $\alpha = 25.4°$ (in the vicinity of the assumed position of the inversion point for the Martian surface) for the spectral range 0.225–0.450 μm. Given the measured value of *B*(25.4°, 0.225 μm), such values of n_r, $\beta(25.4°, 0.225\ \mu m) = \beta_0$, and the particle radius were chosen for the fixed atmospheric pressure that allowed the best description of the spectral variations of $B(25.4°, \lambda)$. As a result, it was found that, at a pressure of 6 mbar near the Martian surface, $n_r = 1.5$–1.6, $\beta_0 = 0.57$–0.61, and the geometric mean of the radii for the lognormal particle-size distribution law $r_0 = 0.051$–0.047 μm at $\sigma^2 = 0.1$, which corresponds to $r_{eff} = 0.065$–0.060 and $\nu_{eff} = 0.11$ for the gamma distribution.

At present, we repeated this study assuming that the refractive index of dust particles varied over the spectrum. Namely, we used the real part of the refractive index provided by Pollack *et al.* (1973) and took the values that we obtained for the maximum of the 1971 dust storm for the imaginary part. The adopted values of n_r and n_i for the wavelengths under consideration are given in Table 3. The optical thickness of the gaseous component τ_g was taken to be equal to 0.02 for a wavelength of 0.335 μm. For other wavelengths, this thickness was determined using the $\tau_g(\lambda) \sim \lambda^{-4}$ law, neglecting the spectral dependence of the gas refractive index. At the first stage, we considered the spheres with sizes distributed by lognormal law (2) with $\sigma^2 = 0.2$. A choice of parameters r_0 and β was made at a phase angle of 25.4°. First, for the wavelength $\lambda = \lambda_0 = 0.225$ μm, we found, using (6)–(9), such values of r_0 and $\beta(\lambda_0)$ for which $|B_{calc}(25.4°)–B_{meas}(25.4°)|/(B_{meas}(25.4°) < 0.1$. Then, these r_0 and $\beta(\lambda_0)$ were utilized to calculate *B*(25.4°) for other wavelengths. For this purpose, we used (6)–(9) and the following relation:

$$\beta(\lambda) = \frac{1}{1 + \frac{1-\beta(\lambda_0)}{\beta(\lambda_0)} \frac{q_{sc}(\lambda)}{q_{sc}(\lambda_0)} \left(\frac{\lambda}{\lambda_0}\right)^4}. \qquad (10)$$

Finally, from the entire set of r_0 and $\beta(\lambda_0)$, we selected those values of the geometric mean of the radii r_0 and β_0 for which the value of $|B_{calc}(25.4°, \lambda) – B_{meas}(25.4°, \lambda)|/B_{maes}(25.4°, \lambda)$ was minimal for all the wavelengths considered.

Table 3. Optical parameters of particles consistent with surface polarization measurements

λ, μm	0.225	0.353	0.376	0.390	0.412	0.434
n_r	1.66	1.58	1.58	1.58	1.57	1.57
n_i	0.0030	0.0011	0.0010	0.0009	0.0008	0.0007
Spheres (r_0 = 0.025 μm, σ^2 = 0.2)						
$\beta^{(1)}$	0.490	0.408	0.396	0.389	0.388	0.380
$\tau_0^{(1)}$	0.200	0.0392	0.0318	0.0280	0.0224	0.0187
$\tau_a^{(1)}$	0.102	0.0232	0.0192	0.0171	0.0137	0.0116
Spheroids (r_0 = 0.04 μm, σ^2 = 0.2, ε = 2.0)						
$\beta^{(2)}$	0.490	0.324	0.302	0.293	0.284	0.271
$\tau_0^{(2)}$	0.200	0.0496	0.0417	0.0374	0.0307	0.0263
$\tau_a^{(2)}$	0.102	0.0336	0.0291	0.0265	0.0220	0.0192
Spheroids (r_0 = 0.05 μm, σ^2 = 0.2, ε = 2.8)						
$\beta^{(3)}$	0.490	0.291	0.268	0.256	0.245	0.231
$\tau_0^{(3)}$	0.200	0.0552	0.0472	0.0427	0.0356	0.0309
$\tau_a^{(3)}$	0.102	0.0392	0.0346	0.0318	0.0269	0.0238

Eventually, we found the geometric mean of the radii r_0 = 0.025 μm, which corresponded to r_{eff} = 0.041 μm and ν_{eff} = 0.22 for the gamma distribution (1). Table 3 demonstrates the obtained spectral values of $\beta(\lambda)$, $\tau_0(\lambda) = \tau_g(\lambda) + \tau_a(\lambda)$, and $\tau_a(\lambda)$ (they are denoted by $\beta^{(1)}$, $\tau_0^{(1)}$, and $\tau_a^{(1)}$) for a pressure of 6 mbar at the Martian surface.

Further, we considered a model of oblate spheroids with the values of the real and imaginary parts of the refractive index of dust aerosol and σ^2 identical to those for spheres. For such particles (applying the same method as for spheres), we found r_0 to be equal to 0.04 μm (r_{eff} = 0.066 μm) at the spheroid axes ratio ε = 2.0 and r_0 = 0.04–0.05 μm (r_{eff} = 0.066–0.082 μm) at ε = 2.8. Table 3 also demonstrates the values of β, τ_0, and $\tau_a(\lambda)$ ($\beta^{(2)}$, $\tau_0^{(2)}$, and $\tau_a^{(2)}$ at r_0 = 0.04 μm and ε = 2.0 and $\beta^{(3)}$, $\tau_0^{(3)}$, $\tau_a^{(3)}$, and $\tau_a^{(3)}$ at r_0 = 0.05 μm and ε = 2.8). As a result, one can see that for dust particles of oblate spheroidal shape the values of both r_0 and τ_0 are somewhat larger than those for the spherical particles; however, they are still much less than the corresponding values obtained, for example, by Pollack *et al.* (1977, 1995).

To check the validity of the estimates obtained for the optical parameters, we used (6) to calculate the phase curves of polarization $P(\alpha, \lambda) = B(\alpha, \lambda)/A(\alpha, \lambda)$ for wavelengths of 0.355, 0.373, 0.413, and 0.459 μm. The visible albedos $A(\alpha, \lambda)$ were taken from observations reported by Irvine *et al.* (1968). Finding the values of $Q_s(\alpha, \lambda)$ ($Q_s(\alpha, \lambda) = -A(\alpha, \lambda)P(\alpha, \lambda)$) appearing in (6) was based on the following approximations: (1) we assumed that $Q_s(\alpha, \lambda)$ was independent of the wavelength; (2) we chose a wavelength of 0.504 μm because for such a wavelength the influence of the atmospheric component could still be ignored and the optical heterogeneity of the underlying surface is already of little importance; (3) we used the measurements of $Q_s(\alpha, \lambda)$ (Irvine *et al.*, 1968) and $P(\alpha, \lambda)$ (Morozhenko, 1975) to calculate $Q(\alpha, \lambda)$ at this wavelength. One can judge the admissibility of the assumption of the wavelength-independent $Q_s(\alpha, \lambda)$ by the data presented in Fig. 2, where the observations of $P(\alpha, \lambda)$ (Morozhenko, 1975) at wavelengths of 0.620 and 0.720 μm are shown by dots, and the calculated values of $P(\alpha, \lambda) = -Q_s(\alpha, 0.504\ \mu\text{m})/A(\alpha, \lambda)$ are denoted by pluses.

The observed phase curves of polarization (see Morozhenko, 1964, 1966, 2000) and the calculated phase curves for wavelengths of 0.355 and 0.413 μm (the scale on the right), as well as for 0.373 and 0.459 μm (the scale on the left), are demonstrated in Fig. 3. The observations are shown by dots, the calculations for spheres with r_0 = 0.025 μm at σ^2 = 0.2 are presented by oblique crosses, and the calculations for oblate spheroids at ε = 2.0, r_0 = 0.04 μm, and σ^2 = 0.2 are denoted by pluses. For phase angles less than 20°, the calculation results for spheres and oblate spheroids are identical to within the accuracy of the figure. It can be seen that the observed polarization agrees well with our calculations performed for polydisperse systems of both spherical and spheroidal particles. Taking into consideration oblate spheroids resulted in a nearly twofold

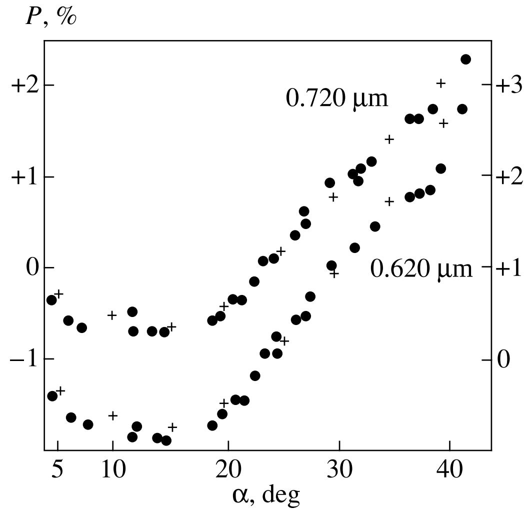

Fig. 2. Phase curves of the polarization of Martian radiation for periods of high transparency of the atmosphere of Mars. Dots correspond to observations; pluses show the calculation results by formula $P(\alpha, \lambda) = -Q_s(\alpha, 0.504\ \mu\text{m})/A(\alpha, \lambda)$.

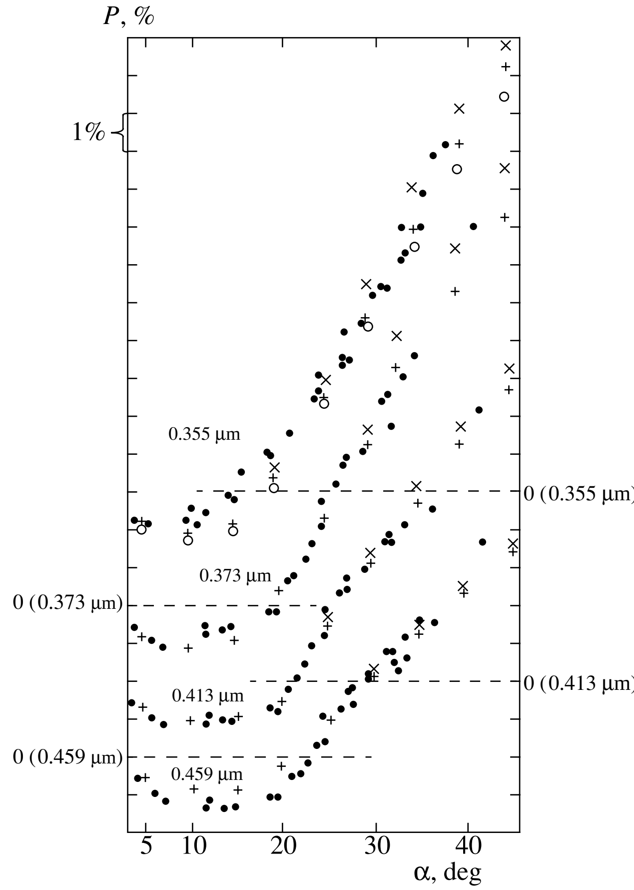

Fig. 3. Phase curves of the polarization of Martian radiation in periods of high transparency of the atmosphere of Mars for wavelengths of 0.355 and 0.413 μm (the scale on the right) and 0.373 and 0.459 μm (the scale on the left). Dots correspond to observations; oblique crosses show calculation results for spheres with r_0 = 0.025μm at σ^2 = 0.2; pluses stand for calculations for oblate spheroids at ε = 2.0, r_0 = 0.04 μm, and σ^2 = 0.2; circles present the calculation results for oblate spheroids at ε = 2.0, r_{eff} = 1.5 μm.

increase in both the mean radius and the optical thickness of the dust layer; however, they still remained much less than the estimates obtained, for example, by analyzing measurements performed on the *Viking 1/2* (Pollack *et al.*, 1977, 1995) and *Mars Pathfinder* (Markiewich *et al.*, 1999; Tomasko *et al.*, 1999) landers.

In addition, we tried to check how well a model of larger particles, considered, for example, by Petrova (1999), agrees with surface polarization observations. For this purpose, we adopted a model of spheroidal dust particles with size distribution obeying the modified power law with r_{eff} = 1.5 μm, n_r = 1.5, and n_i = 0.001 (see the preceding section). For a wavelength of 0.353 μm, we found that the minimum of $|B_{\text{calc}}(25.4°) - B_{\text{meas}}(25.4°)|/B_{\text{meas}}(25.4°)$ (it was found to be 0.27) is attained at β = 0.8; that is, τ_0 = 0.02 (τ_a = 0.004, respectively). Note that similar small optical thicknesses (for another model) were obtained by Tishkovets and Shkuratov (1982). Thus, the optical thickness found for the dust layer proved to be even smaller than that for the particles considered above. The circles in Fig. 3 demonstrate the calculated phase curve of polarization for such particles at a wavelength of 0.355 μm. It is clear that they agree less well with the observations. From our point of view, this can indicate that the model of oblate spheroids with r_{eff} = 1.5 μm and n_r = 1.5 cannot be used for the interpretation of surface polarization observations.

Thus, we have demonstrated that the choice of dust particle shape affected the estimates of optical parameters based on analyzing polarization and photometric observations. The introduction of the model of spheroidal dust particles resulted in increases in mean radii r_0 and optical thicknesses τ_0 of the dust layer during the periods of high transparency of the Martian atmosphere by a factor of approximately two as compared to the model of spherical dust particles. The same is also true for the estimates of the imaginary part n_i of the refractive index as inferred from photometric observations during the maximum of the dust storm in 1971. However, the obtained values of these optical parameters are still much less than the corresponding estimates found by other authors by analyzing the results of space experiments. In our view, the cause of this mismatch remains unclear and needs further consideration.

ACKNOWLEDGMENTS

In conclusion, we would like to thank V.I. Moroz for the discussions that initiated this study, and the reviewer for useful remarks.

REFERENCES

Aleksandrov, Yu.V., Lupishko, D.F., and Lupishko, T.A., *Absolyutnaya fotometriya Marsa v 1971, 1973, 1975 godakh* (Absolute Photometry of Mars in the Years 1971, 1973, and 1975), Kharkov: Vysshaya Shkola, 1977.

Caldwell, J., Ultraviolet Observations of Mars and Saturn by the *TDIA* and *OAO-2* Satellites, *Icarus*, 1977, vol. 32, no. 2, pp. 190–209.

Dlugach, Zh.M., Method and Results of Calculations of the Optical Properties of the Martian Atmosphere during the Period of the 1971 Global Dust Storm, *Astrometriya i Astrofizika*, 1978, no. 30, pp. 50–64.

Dlugach, J.M. and Yanovitskij, E.G., The Optical Properties of Venus and the Jovian Planets. II. Methods and Results of Calculations of the Intensity of Radiation Diffusely Reflected from Semi-infinite Homogeneous Atmospheres, *Icarus*, 1974, vol. 22, no. 1, pp. 66–81.

Dlugach, Zh.M. and Morozhenko, A.V., Aerosol in the Martian Atmosphere, *Kinematika Fiz. Nebesnykh Tel*, 2000, vol. 16, no. 5, pp. 437–453.

Dlugach, Zh.M. and Morozhenko, A.V., Parameters of Dust Particles in the Martian Atmosphere, *Astron. Vestn.*, 2001, vol. 35, no. 6, pp. 467–478 [*Solar Syst. Res.* (Engl. transl.), 2001, vol. 35, no. 6, pp. 421–430].

Dollfus, O., Dlugach, J.M., Morozhenko, A.V., and Yanovitskii, E.G., Optical Parameters of the Atmosphere and Surface of Mars: II. Dust Storms, *Astron. Vestn.*, 1974, vol. 8, no. 4, pp. 211–222.

Irvine, W.M., Simon, T., Menzel, D.H., *et al.*, Multicolor Photoelectric Photometry of the Brighter Planets: III. Observations from Boyden Observatory, *Astron. J.*, 1968, vol. 73, no. 9, pp. 807–828.

Markiewich, W.I., Sablotny, R.M., Keller, H.U., *et al.*, Optical Properties of the Martian Aerosols as Derived from Imager for *Mars Pathfinder* Midday Sky Brightness Data, *J. Geophys. Res.*, 1999, vol. 104, no. E4, pp. 9009–9017.

Mishchenko, M.I., Travis, L.D., and Mackovski, D.V., T-Matrix Computations of Light Scattering by Nonspherical Particles: A Review, *J. Quant. Spectrosc. Radiat. Transfer*, 1996, vol. 55, no. 5, pp. 535–575.

Mishchenko, M.I. and Travis, L.D., Capabilities and Limitations of a Current Fortran Implementation of the T-Matrix Method for Randomly Oriented Rotationally Symmetric Scatterers, *J. Quant. Spectrosc. Radiat. Transfer*, 1998, vol. 60, no. 3, pp. 309–324.

Morozhenko, A.V., Results of Polarimetric Observations of Mars in 1961–1963, in *Fizika Luny i planet* (Physics of the Moon and Planets), Kiev: Naukova Dumka, 1964, pp. 58–80.

Morozhenko, A.V., Polarization Properties of the Atmosphere and Surface of Mars, in *Fizika Luny i Planet* (Physics of the Moon and Planets), Kiev: Naukova Dumka, 1966, pp. 45–69.

Morozhenko, A.V., The Martian Atmosphere from Polarization Observations, *Astron. Zh.*, 1969, vol. 46, no. 5, pp. 1087–1094.

Morozhenko, A.V., Optical Parameters of the Atmosphere and Surface of Mars: I. Aerosol Composition of Clear Atmosphere, *Astron. Vestn.*, 1974, vol. 8, no. 3, pp. 121–127.

Morozhenko, A.V., Results of Polarimetric Observations of Mars in 1971 and 1973, *Astrometriya i Astrofizika*, 1975, no. 26, pp. 97–107.

Morozhenko, A.V., Physical Properties of the Martian Atmosphere during the Periods of Dust Storms: I, *Kinematika Fiz. Nebesnykh Tel*, 1995a, vol. 11, no. 1, pp. 32–48.

Morozhenko, A.V., Physical Properties of the Martian Atmosphere at Periods of Dust Storms: II, *Kinematika Fiz. Nebesnykh Tel*, 1995b, vol. 11, no. 3, pp. 3–19.

Morozhenko, A.V., Results of Spectrophotometric Observations of Planets and Jupiter's Galilean Satellites at the 1986, 1988, and 1989 Oppositions: II, *Kinematika Fiz. Nebesnykh Tel*, 2001, vol. 17, no. 1, pp. 45–57.

Murphy, J.R., Toon, O.B., Haberle, R.M., and Pollack, J.B., Numerical Simulations of the Decay of Martian Global Dust Storms, *J. Geophys. Res.*, 1990, vol. 95, no. B9, pp. 14 629–14 648.

Ockert-Bell, M.E., Bell II, J.F., Pollack, J.B., *et al.*, Absorption and Scattering Properties of the Martian Dust in the Solar Wavelengths, *J. Geophys. Res.*, 1997, vol. 101, no. E4, pp. 9039–9050.

Petrova, E.V., Mars Aerosol Optical Thickness Retrieved from Measurements of the Polarization Inversion Angle and the Shape of Dust Particles, *J. Quant. Spectrosc. Radiat. Transfer*, 1999, vol. 63, nos. 2–6, pp. 667–676.

Pollack, J.B., Toon, O.B., and Khare, R., Optical Properties of Some Terrestrial Rocks and Glasses, *Icarus*, 1973, vol. 19, no. 3, pp. 372–383.

Pollack, J.B., Colburn, D.S., Khan, R., *et al.*, Properties of Aerosols in the Martian Atmosphere as Inferred from *Viking* Lander Imaging Data, *J. Geophys. Res.*, 1977, vol. 82, no. 28, pp. 4479–4496.

Pollack, J.B., Ockert-Bell, M.E., and Shepard, M.K., *Viking* Lander Image Analysis of Martian Atmospheric Dust, *J. Geophys. Res.*, 1995, vol. 100, no. E3, pp. 5235–5250.

Thorpe, Th.E., *Mariner 9* Photometric Observations of Mars from November 1971 through March 1972, *Icarus*, 1973, vol. 20, no. 4, pp. 482–489.

Tishkovets, V.P. and Shkuratov, Yu.G., On the Polarization Properties of the Surface and Atmosphere of Mars, *Astron. Zh.*, 1982, vol. 59, no. 5, pp. 991–995.

Tomasko, M.C., Doose, L.R., Lemmon, M., *et al.*, Properties of Dust in the Martian Atmosphere from the Imager on *Mars Pathfinder, J. Geophys. Res.*, 1999, vol. 104, no. E4, pp. 8987–9007.